Spectroscopy of ^{34,35}Si by β decay: $sd-fp$ shell gap and single-particle states

S. Nummela, P. Baumann, E. Caurier, P. Dessagne, A. Jokinen, A. Knipper, G. Le Scornet, C. Miehe, F. Nowacki, M. Oinonen, et al.

EUROPEAN ORGANIZATION FOR NUCLEAR RESEARCH

CERN-EP/2000-073
16 May 2000

Spectroscopy of ^{34,35}Si by β decay : sd-fp shell gap and single-particle states

S. Nummela[1,2], P. Baumann[3], E. Caurier[3], P. Dessagne[3], A. Jokinen[1,2], A. Knipper[3], G. Le Scornet[4], C. Miehé[3], F. Nowacki[5], M. Oinonen[6], Z. Radivojevic[1], M. Ramdhane[7], G. Walter[3], J. Äystö[1,6] and the ISOLDE Collaboration

[1]Department of Physics, University of Jyväskylä, P.O. Box 35, Jyväskylä, Finland
[2]Helsinki Institute of Physics, University of Helsinki, Finland
[3]IReS, IN2P3-CNRS, Louis Pasteur University, BP 20 F-67037 Strasbourg Cedex, France
[4]CSNSM, 91405 Campus Orsay, France and EP-Division, CH-1211 Geneva, CERN, Switzerland
[5]Theoretical Physics Laboratory, F-67084 Strasbourg Cedex, France
[6]EP-Division, CH-1211 Geneva, CERN, Switzerland
[7]University of Constantine, Constantine, Algeria

Abstract

The ^{34,35}Al β decays were studied at the CERN on-line mass separator ISOLDE by β-γ, β-γ-γ and β-n-γ measurements, in order to corroborate the low-level description of ^{34}Si and to obtain the first information on the level structure of the N=21 isotope ^{35}Si. Earlier observed γ lines in ^{34}Al decay were confirmed and new gamma transitions following both beta decay and β-delayed neutron emission were established. The first level scheme in ^{35}Si, including three excited states at 910, 974 and 2168 keV, is consistent with $J^{\pi}= \frac{3}{2}^{-}$and $\frac{3}{2}^{+}$ for the first two states respectively. Beta-decay half-life of $T_{\frac{1}{2}}$=38.6 (4) ms and beta-delayed neutron branching P_n value (P_n=41(13) %) were measured unambiguously. The significance of the single-particle energy determination at N=21, Z=14, for assessing the effective interaction in sd-fp shell-model calculations, is discussed and illustrated by predictions for different n-rich isotopes.

submitted to Physical Review C

I. INTRODUCTION

Recently, several independent measurements concerning the study of neutron-rich nuclei located near the N=20 and N=28 shell closures (Z=20), have been carried out with different approaches and techniques [1–5]. The vast interest for this region dates back to a measurement by Thibault et al. [6] when a region of strong deformation was discovered around Z=11, N=20, not expected by the sd shell model. At the present time, the available experimental data on masses, level structure and transitions probabilities [7–10] have initiated refined theoretical calculations [11–20] concerning different configurations around the N=20 shell closure. It has already been shown through beta-decay studies that ^{34}Si lies at the edge of this deformed island [21] in the (N,Z) plane, having a 0p-0h ground state, while its two lowest excited states have a large fp-shell intruder component.

Recent measurements of B(E2) values and the location of 2_1^+ states performed at MSU [2] for even $^{28-32}$Si isotopes indicate a similar result, and by assuming the N=20 neutrons as a closed shell for N>20 silicon isotopes, the experimental 2_1^+ states can be reproduced. An additional source of information on the interplay between $0\hbar\omega$ and $2\hbar\omega$ states at N=20 would be the experimental confirmation of a 0_2^+ intruder state at low energy in ^{34}Si. This was the first goal of the present work. The second one was to obtain the low energy level structure of the N=21 ^{35}Si isotope. As a matter of fact, in shell-model studies, the evolution of single-particle energies plays an important role in determining the effective interactions between valence particles. With the experimental data on the first excited states of ^{35}Si (N=21), which up to now has been unknown, we can extend the test of the evolution of single-particle $p_{\frac{3}{2}}$ and $d_{\frac{3}{2}}$ states of N=21 isotones starting from Z=20 (^{41}Ca) down to Z=14 (^{35}Si).

Motivated by these basic questions for the shell-model predictions around N=20, we carried out an experiment concerning the beta-decay study of ^{34,35}Al at CERN, using the ISOLDE on-line separator. The results will be discussed in the framework of a shell-model calculation performed in the full (sd-fp) space. Preliminary results of the present work have been reported in [22,23].

II. EXPERIMENTAL PROCEDURES

^{34,35}Al activities were produced at the ISOLDE facility at CERN in fragmentation reactions with a pulsed 1 GeV proton beam from the PS-Booster impinging on a uranium carbide target with a thickness of 46 g cm^{-2} for U. The intensity of the proton beam was 3 $\times 10^{13}$ ions/pulse, the time interval between pulses being a multiple of 1.2 s and the average beam current was above 2μA. The reaction products were ionized in a tungsten surface-ionization source and separated by mass. With this target-ion source device, the highest yield corresponds usually to alkalis. However, in the mass range 33<A<35, the Na isotopes give a minor contribution to the radioactive beam, the essential part of it being given by the directly produced Al isotopes. The yield for mass-separated ^{34}Al isotopes was 30 atoms/s while for ^{35}Al it was close to 10 atoms/s. Ions were collected onto a tape which was moved periodically in order to reduce the amount of contaminants and longer lived daughter activities. The experimental set up, which was assembled around the collection point, was suited for detecting beta particles, gamma rays and beta-delayed neutrons. A thin cylindrical plastic detector, covering a large fraction of the total solid angle around the collection point, was used for triggering beta-gamma coincidences and provided a start signal for neutron time of flight measurements. Two large-volume Ge detectors recorded gamma rays both as beta-gamma coincidences as well as beta-gamma-gamma coincidences. For beta-delayed neutron time of flight measurements, 8 low-threshold neutron detectors were located around the collection point with a similar flight path of 45 cm. These detectors were small plastic scintillator counters (1 cm thick, diameter 10 cm) each viewed by two phototubes XP2020 operated in coincidence, as described in Ref. [24]. Their intrinsic efficiency is about 15 % and the variation of the efficiency with the neutron energy was evaluated during the same run by measuring the delayed-neutron spectrum of ^{29}Na for which the relative intensity of the neutron branches have been measured previously [25,26].

For both masses, A=34 and 35, two gamma spectra were created, during acquisition and during off-line analysis, corresponding to two time windows of the separator beam-pulsing cycle. This provided a clear identification of gammas following the beta decay of ^{34}Al and ^{35}Al from those of the precursors (Na or Mg) and of multiple-charged ions (as an example ^{140}Xe, 4$^+$for A=35) due to the difference in lifetimes. Half lives were determined by fitting intensity of betas and gammas taken in 5 ms time bins during the decay part of the radioactive beam cycle, resulting in a unambiguous half-life information.

The decay schemes were extended according to gamma-gamma coincidences for the most intense gammas, and in some weaker cases according to pure gamma singles not in contradiction with the intensity analysis in coincidence spectra. Finally, some limits for level lifetimes could be determined from the beta gamma-delayed coincidences measured with plastic and Ge detectors enabled to restrict the multipolarity of the corresponding transitions and accordingly spin and parity assignments for some of the levels. In the particular case of the ^{35}Si level scheme, we

decided to investigate the beta-gamma coincidences with improved time resolution. In a separate experiment, we used the delayed-coincidence technique with the thin plastic scintillator and a small BaF_2 counter (conical shape, 2.5 and 2.0 cm diameter, 2.5 cm height) optically coupled to a XP2020/Q phototube.

III. RESULTS

A. Beta-decay of ^{34}Al

By comparison with the first study of ^{34}Al [21], employing the SC beam at 600 MeV, the improvement of the production yield with the pulsed 1 GeV beam in this experiment corresponds to a factor 3 and allows a better description of the ^{34}Al decay. The half life is determined as $T_{1/2}$=56.3(5)ms, weighted average of 55.6(1.3)ms from the strongest gamma transitions, and 56.4(6)ms from β-multiscaling. Based on γ-γ coincidences the previously reported four gamma transitions following the beta decay of ^{34}Al are confirmed together with spin and parity assignments in the ^{34}Si level scheme [21]. In addition to the known transitions, one new γ transition with energy of 591 keV is found in coincidence with γ lines of 124, 929 and 3326 keV energy, which places the transition above the 4379 keV level. Four new gamma rays are found in the γ-single spectra which can be assigned to the ^{34}Al beta decay according to the half-life analysis. One of these transitions, with 1053 keV energy, is placed in the level scheme of ^{34}Si due to energy difference of the 4379 and 3326 keV levels. The transitions and their intensity are listed in Table I.

The 1435 keV transition can be placed in the ^{33}Si level scheme, resulting from beta-delayed neutron emission, on the ground of two observations. First, a weak 1435 keV line can be seen in coincidence with neutrons and secondly, this line cannot be observed in coincidence with high-energy betas refering to a low Q value (S_n=7.53 MeV in the case of ^{34}Si). An additional indication is found in the literature, as this energy has been attributed to a 1435 $\rightarrow$ 0 keV transition in the ^{33}Si level scheme, in heavy-ion induced reaction studies [27,28]. From these previous works, $J^\pi=7/2^-$has been proposed for the 1435 keV level. The population of a $7/2^-$state in the beta decay of ^{34}Al ($J^\pi=4^-$) is very likely as resulting from the deexcitation of the $(3,4)^-$states, populated by GT transitions, through an l=0 neutron emission.

The branch at 1010 keV was too weak to be observed in coincidence with neutrons. Nevertheless, as the same energy has been reported in ^{33}Si by Fornal et al. [27] in deep-inelastic studies, we have a tentative evidence for a transition following neutron-delayed emission.

In our β-γ spectrum there can be seen lines corresponding to the ^{33}Si beta decay, consecutive to the beta-delayed neutron emission of ^{34}Al. Assuming the beta branch from ^{33}Si ($J^\pi=3/2^+$) to the ^{33}P ground state ($J^\pi=1/2^+$) negligible (see Ref. 13), we can determine the P_{1n} value from the relative intensity of the ^{33}Si and ^{34}Al filiations. This leads to a P_{1n} value of 26(4)% which is in good agreement with the one obtained by Baumann et al. (27(5)%) [21] in a previous experiment and using the same technique. However, the discrepancy is large compared to the value (P_n=54(12)%) reported by Bazin et al. [29] and by Reeder et al. (P_n=12.5(25)%) [3,10] using different techniques. In our data, there is no sign of gamma lines belonging to the ^{32}Si level scheme and therefore there is no indication for a beta-delayed 2n emission.

According to our data and using the Q-beta value given in Ref. [10], a revised decay scheme of ^{34}Al is established and reported in Fig. 1. In the previous beta-decay measurement of ^{34}Al [21], the ground state, the first and the second observed excited state at 3326 keV and 4255 keV have been reliably assigned $J^\pi=0^+$, $2^+$and 3^-. For the 4379 keV state the assignment is 3^-, 4^- or 5^- due to the allowed nature of the decay of the $J^\pi=4^-$ground state of ^{34}Al. The new logft values and beta branchings are shown in Table II. They confirm the spin and parity assignments stated before. Also, the new state at 4970 keV can only be considered as 3^-, 4^- or 5^-.

The most important new piece of information on the ^{34}Si level scheme is the observation of gamma lines among which a candidate for a transition to the first excited 0^+ state can be found. This level is predicted below the first 2^+ and in this experiment we foresee no beta feeding but only a gamma population from the 2_1^+ level. The $2_1^+ \rightarrow 0_2^+$branching is expected to be only a few percent, as the competing $2_1^+ \rightarrow 0_1^+$ transition is favoured by the energy factor. In the gamma spectra gated by the 2_1^+ feeding, we did not reach an adequate level of sensitivity and no candidates could be found in the gamma-coincidence spectra with our statistics. Therefore we consider the lines in the beta-gamma spectra, decaying with a rate compatible with the ^{34}Al half life in order to locate the $2_1^+ \rightarrow 0_2^+$ transition and we are left with two possible candidates : 1193 and 1715 keV. These lines would correspond, respectively, to transitions from 3326 (2_1^+) to levels at 2133 or 1611 keV.

The extraction of gamma-branching ratios from the β-γ coincidence data, in the particular case of the feeding of an excited 0^+ state, should take into account the sequence of the emitted radiations. In the following, we describe the adopted procedure in the case of the 1193 keV/3326 keV intensity ratio.

A 0^+ excited state, postulated at 2133 keV, will decay predominantly by pair emission, e^+e^- with a probability of P_π. We calculate from Wilkinson [30,31] that $P_\pi/P_e = 49$, P_e being the probability of atomic electron emission. In this case, our β-γ detection device, used for the intensity measurements reported in Table I, can be triggered by any of the two electrons emitted as well as by the first beta. If the beta-detection probability for a single event is called P, it will amount to $3P(1-P)+P^3$ for the higher multiplicity event corresponding to a pair emission consecutive to a beta transition. In our conditions, we estimate an increase of the detection efficiency by a factor 2.00(25) for the β-γ event associated to the pair emission. The relative intensity of the 1193 keV transition, reported as 6.4(8) in Table I, should be 3.2(6) if this transition populates the 0_2^+ level.

A similar correction can be made in the case of the 1715/3326 ratio. For the 1715 keV, we calculate $P_\pi/P_e = 9.5$.

From the discussion and the comparison with estimates which are reported in the next section (see IV. Discussion), we are lead to select the 1193 keV line as the best candidate for a (2_1^+,E_X = 3326 keV $\rightarrow$ 0_2^+,E_X = 2133 keV) transition. However, we have no information from the present experiment on gammas emitted in coincidence with the 1193 keV line and therefore the proposed assignment has to be verified. For the 1715 and 2696 keV lines, for which no coincidence relation were found, no placement in the level scheme could be proposed.

B. Beta decay of ^{35}Al

So far no indications were available about the beta-decay branches of ^{35}Al. The half life has been reported as 150(50) ms [32] and later 30(4) ms [3,10] but no gamma transitions have been observed. In the present experiment, the half life could be measured from the beta-counting rate as well as from the decay of the strongest gamma transitions, as represented in Fig. 2. Taking the average of three independent beta and one gamma measurement, we obtain the weighted mean (and adopted) value of 38.6(4) ms. The two strongest lines, with energy of 64 and 910 keV, were clearly detected in coincidence, as can be seen in Fig. 3, where their coincidence spectrum and the evolution of these lines in two time bins are presented.

In addition, three more transitions were observed in the singles-gamma spectra and could be assigned to ^{35}Al decay on the basis of their decay rate. The 974 keV line corresponds to a cross-over transition of the cascade 64-910 keV and the 2169 keV transition is attributed to a branch to the ground state from a level at this energy. Finally, the energy difference between the 2169 and the 974 keV levels corresponds to the third transition : 1194 keV. This line, measured in the A=35 experiment at 1194.2(3) keV, should be distinguished from the line we reported at 1193.3(2) keV in the A=34 study (Table I). The transitions assigned to the ^{35}Al decay and their intensity are listed in Table III together with three transitions belonging to the ^{34}Si level scheme following beta-delayed neutron emission.

The P_n value for ^{35}Al is obtained by measuring the relative intensities of the ^{34}P and ^{35}P activities, as we know that these isotopes are only present as daughter products of the ^{35}Al decay. The resulting P_n value (41(13)%) is found larger than the value reported previously by Reeder et al. [3,10] (P_n=26(4)%) but in excellent agreement with the result of Lewitowicz et al., P_n=40(10)% [32,33]. No evidence was found for any A=33 activity and 2n emission was then found negligible (the 2n-emission energy window is equal to 4.3 MeV).

The energy spectrum of the delayed-neutron emission of ^{35}Al was measured by time of flight on the 45 cm flight path. The resulting spectrum is given in Fig. 4 with the ^{29}Na delayed-neutron spectrum, taken in the same experiment and used for detection efficiency control. Despite the small solid angle covered by the neutron detectors in this experiment, dominated by prompt beta-gamma coincidences, two maxima can be observed around 3.0 MeV and 0.98 MeV. The quantitative evaluation of the absolute intensity of these distributions is difficult as we have to make an assumption for the fraction of the neutron spectrum located below the threshold. Nevertheless, if we take into account the large fraction of the gamma rays consecutive to the neutron emission, the neutron energy spectrum reveals that the range of the excited levels involved in this process can approximately be traced up to 8 MeV.

The beta branch to the ^{35}Si ground state has been evaluated by comparing the gamma intensity corresponding to the ^{35}Si excited states deexcitation with the ^{35}Si activity and assuming no direct production of ^{35}Si by the beam. The value deduced from our experiment (3 %) is found compatible with the first-forbidden character of this transition. Taking into account the new P_n value and the Q-beta deduced from Ref. [10], logft values and beta-branching values are calculated and reported in Table IV.

In our interpretation of the ^{35}Al β decay, we shall assume that ^{35}Al (Z=13, N=22) g.s. has $J^\pi=5/2^+$, as expected from the systematics in Al isotopes.

According to the logft values, a decay branch from the ^{35}Al $J^\pi=5/2^+$state to the 974 keV level in ^{35}Si is considered as an allowed GT decay. From general shell-model considerations, the first positive parity state in the N=21 ^{35}Si nucleus, results from a 1p-1h configuration, with a $d_{3/2}$ neutron hole. We propose then $J^\pi=3/2^+$ for the 974 keV level which will be discussed in more detail in the next section. With the same simple shell-model considerations, we propose for the ^{35}Si ground state a $J^\pi=7/2^-$ value (which is in agreement with the ^{35}Si $\rightarrow$ ^{35}P decay) and $J^\pi=3/2^-$

for the first excited state as expected from the N=21 isotone systematics and from the weak beta feeding. We have then the sequence $7/2^-$, $3/2^-$, $3/2^+$ for the three first levels corresponding to a cascade with the 64 and 910 keV lines in an order which has to be determined.

Since the intensities of the 64 keV and 910 keV energy gamma transitions are equal within error limits, their order has to be deduced from level-lifetime considerations. As the lowest transition implies a quadrupole character ($3/2^- \rightarrow 7/2^-$), an energy of 64 keV would correspond to a lifetime in the microsecond range. Such a lifetime was not observed, and therefore the 64 keV transition is placed above the 910 keV transition. This places the first excited state at 910 keV. The information obtained from this experiment and the values deduced from the present discussion are reported in Fig. 5, which is the first decay scheme established for ^{35}Al. Beta and gamma transitions are coherent with the proposed J^π values for the ^{35}Si levels. The $3/2^+$ level, which has a strong beta feeding, is decaying to the ground state by an M2 transition which is in competition with the presumed E1 transition ($3/2^+ \rightarrow 3/2^-$, 64 keV). The relative intensity of these two radiative decays is found in good agreement with the usual width of M2 and E1 transitions. According to the logft value, the spin value of the 2168 keV level is limited to $J^\pi = (3/2 - 7/2)^+$. The value reported in Fig. 5 ($J^\pi = (5/2)^+$) results from the comparison with the B(GT) calculation given in the next section. The relative intensity of the two decay branches of the 2168 keV $(5/2)^+$ level, are compatible with two transitions, mostly E1 and M1 transitions.

An additional evidence for the assignments proposed for the low levels of ^{35}Si has been given by a measurement of the 974 keV, $(3/2^+)$ level lifetime. With the energies and multipolarities involved, this lifetime was estimated to be in the range of the delayed-coincidence technique and able to give a test of our hypothesis, for the two transitions depopulating this level, of a magnetic quadrupole radiation in competition with a low energy electric dipole. The lifetime of the ^{35}Si, $J^\pi = 3/2^+$ was then measured in a separate experiment.

The coincidences detected with the thin plastic beta counter and the BaF_2 scintillator were registered as bi-parametric events E_γ-t. The time spectrum corresponding to prompt events was determined with a ^{22}Na source. With the ^{35}Al beam, it was found that the 64 keV line, as well as 910+974 lines (not resolved with the BaF_2 counter), gave delayed events in the time spectra. This result revealed the order of the cascade, with the measurable lifetime assigned to the 974 keV level, delaying all consecutive transitions with regard to the beta detection. The analysis of the time spectrum was made by selecting events in time and energy ranges as follows :

- the energy range excluded the lowest part of the spectrum, for which time properties were found poorly defined.

- the time range excluded the portion corresponding to prompt events as defined with the ^{22}Na source.

After a careful determination of the background of the time spectrum in the selected interval, the analysis done on the delayed events of the coincidence curve leads to the value for the lifetime τ of the 974 keV level : $\tau = 8.5(9)$ ns.

In Figure 6, we have reported the prompt- and delayed- time spectra and indicated the range of the analysis. The intensity of prompt events in the A=35 spectrum can be interpreted with events corresponding to large energy betas firing both detectors. Taking into account the branching ratio (974 keV (11 %), 64 keV (89 %)), we can express the result for the two partial widths in Weisskopf units, which yields : , /, $_W$=0.35(4) 10^{-3} for the 64 keV, E1 transition and , /, $_W$=0.061(7) for the 974 keV, M2 transition. These values are found in the range of the experimental results for similar transitions in light nuclei (see for example [34]). We conclude then that the different observables which could be obtained in the ^{35}Al decay give supporting evidence for the proposed decay scheme.

IV. DISCUSSION

A. Derivation of sd-fp shell model interaction

From the shell-model point of view, nuclei of interest belong to the sd-fp valence space. It was demonstrated in [20] and then confirmed in [35,36], that protons remain in the sd shell. On the other hand, for neutrons, there will be a competititon between $0\hbar\omega$ configurations (filling (sd) for N<20 and (fp) for N>20) and intruder configurations (sd $\rightarrow$ fp excitations).

In [19], an effective interaction was build for this valence space ; it contained three parts, the USD matrix elements [37] from proton-proton interaction, the KB' matrix elements [38] for the neutron-neutron interaction and the G matrix of Kahana, Lee and Scott (KLS) [39] for the proton-neutron matrix elements. This latter was modified, through its monopole terms, to reproduce the evolution of the $\frac{3}{2}^+$, $\frac{1}{2}^+$doublet along K isotopes and the position of $\frac{5}{2}^+$ in ^{47}K.

As already mentioned at that time, these experimental data are not sufficient to fix all the monopole parameters and the spectrum of ^{35}Si was (partially arbitrarily) adjusted on the ^{41}Ca one. The evolution of proton-hole states

in potassium isotopes fixes essentially the difference between $f_{\frac{7}{2}}d_{\frac{3}{2}}$ and $f_{\frac{7}{2}}s_{\frac{1}{2}}$ monopoles (neutrons occupy almost only $f_{\frac{7}{2}}$ shell in K isotopes). So we will let these terms unchanged. The evolution of the single-neutron states from ^{41}Ca to ^{35}Si is governed by the remaining cross monopoles (see Fig. 7): we will act only on $p_{\frac{3}{2}}s_{\frac{1}{2}}$ and $p_{\frac{3}{2}}d_{\frac{3}{2}}$ to reproduce the evolution of the $\frac{3}{2}^-$state. The position of the $\frac{3}{2}^-$ state in the N=21 isotones is given in Fig. 8 resulting from experiments and calculations. According to our data on ^{35}Si the effective interaction was modified and gives a global agreement for the N=21 isotones from Z=14 to Z=20.

B. Influence on the physics of sd-fp nuclei

The new observed single-particle states in ^{35}Si can be interpreted as a reduction of the neutron gap between $f_{\frac{7}{2}}$ and $p_{\frac{3}{2}}$ shells or an erosion of the spin-orbit force far from stability. This erosion is moderate but it is of interest to analyse its consequences, in particular going from the N=20 region to the N=28 shell gap.

In this intention, a new calculation of the Z<20, N>20 nuclei was made for comparison with our previous estimates [19]. In Table V we give results for even-even n-rich nuclei where comparison with experiment is available. Most of the effect is really moderate with minor incidences : we report the example of ^{40}Ar and ^{40}S where the electromagnetic transition properties remain unchanged. For the N=28 isotones, Table V indicates minor changes again except in the case of ^{42}Si where the double-closed shell character from the study [19] is much less pronounced. This nucleus is very unstable with respect to the choice of the interaction. The explanation is that it lies in the transition region between the N=28 gap persistence (^{46}Ar, ^{44}S) and the vanishing of the shell closure ^{40}Mg [20].

One of the aspects which was not emphasized in [19] is the occurence of shape coexistence (spherical/prolate) at N=28. This has been recently observed and analysed in the two experiments where the observation of an isomeric state in ^{43}S [5] and the Coulomb excitation measurement of ^{43}S [4] sign the coexistence of spherical and deformed shapes in this nucleus. As explained in Ref. 40, the deformation effect is essentially due to protons, but it is enhanced by the reduction of the $f_{\frac{7}{2}}$-$p_{\frac{3}{2}}$ neutron gap observed in ^{35}Si. Fig. 9 presents the observed properties of ^{43}S [4,5] compared with calculations using the interaction deduced from the present study.

C. GT transitions and intruder states in ^{34}Si

The beta decay scheme of ^{34}Al resulting from the present work confirms and completes the first study [21]. We report beta branches to three excited states which are interpreted as negative parity particle-hole states in ^{34}Si.

We have reported in Fig. 10 (left part), the theoretical distribution of the Gamow-Teller strength corresponding to the three possible values of $J^\pi = (3, 4, 5)^-$ for the final states in ^{34}Si. The total strength is very similar in the three cases, with a broad distribution peaking around 23 MeV, above the Q_β window. The low energy part reveals interesting features : two $J^\pi=4^-$ levels, between 4 and 5 MeV, are predicted to be populated by strong GT transitions. Comparing experiment (Fig. 1) with these results, it is seen an excellent agreement for the distribution of the allowed transitions.

A further test of the calculations would be given by the properties of the first two $0^+$and 2^+states, as already discussed in Ref. [20], allowing a detailed description of normal and intruder, 2p-2h states. From these four levels, only two (0_1^+ and 2_1^+) are known. A second 2^+ can be tentatively associated with a level at 5.3 MeV [28]. From the present work, a plausible candidate for the 0_2^+ level is proposed at 2133 keV, as the 1193 keV transition was tentatively associated with the $2_1^+ \rightarrow 0_2^+$transition. In this line, it is of interest to compare the relative intensity of the 1193 and 3326 keV gamma rays with the expected value for the $2_1^+ \rightarrow 0_2^+$ and $2_1^+ \rightarrow 0_1^+$ transitions.

If the 3326 and 1193 keV transitions correspond to the two decay branches ($2_1^+ \rightarrow 0_1^+$ and $2_1^+ \rightarrow 0_2^+$) of the 2_1^+ level we can estimate the B(E2↑) ($0_2^+ \rightarrow 2_1^+$) value, using the corrected value (3.1(6)) for the branching ratio and the experimental result (B(E2↑) = 85(33)e^2fm^4) given previously by Ibbotson et al. [2] for the $0_1^+ \rightarrow 2_1^+$ transition. After correction by the energy factor, we find : B(E2↑) ($0_2^+ \rightarrow 2_1^+$) = 444(210) e^2fm^4. This latter result is consistent with the hypothesis of a 0_2^+, $2\hbar\omega$ state, at 2133 keV and strongly connected to the 2_1^+, $2\hbar\omega$ state.

In Table VI, we have reported energy and B(E2) values, calculated for the three first levels of ^{34}Si. We have indicated experimental results which can be compared. We conclude that the experimental results are close to those expected but a confirmation of the location of the 0_2^+ level is still needed.

How does the 1715 keV transition compare to the 1193 keV one as a $2_1^+ \rightarrow 0_2^+$ candidate ? It would imply a 0_2^+ level at 1611 keV. Using the intensity measurement and the B(E2↑)($0_1^+ \rightarrow 2_1^+$) value, as described for the 1193 keV transition, one would get : B(E2↑) ($0_2^+ \rightarrow 2_1^+$) = 27(12) e^2fm^4, well below the expected value. This result is not consistent with predictions for a $2\hbar\omega$ state, even with mixing assumed.

D. GT transitions in ^{35}Si

The allowed transitions reported in the ^{35}Al decay scheme (Fig. 5) can be compared with the results of the sd-fp calculations reported in the right part of Fig. 10. In the three GT-strength distributions, corresponding to the final spin values, only the low energy part is relevant for this comparison. A marked feature is that only two transitions are predicted in the range of ^{35}Si bound levels (S_n=2.47 MeV). The $3/2^+$state is in excellent agreement with the observed 974 keV level. The first $5/2^+$is predicted slightly higher than 2.17 MeV but can clearly be associated with it. Between 6 and 8 MeV ^{35}Si excitation energy, a complex of levels given by the calculation, allows to understand the main features of the beta-delayed-neutron spectrum (Fig. 4). Among these, the $7/2^+$ levels predicted by the calculation are the best initial state candidates for transitions to ^{34}Si, 2_1^+ final state. For these neutrons indeed, an l = 4 channel spin is required for the emitted neutron populating ^{34}Si g.s. and only l = 2 for ^{34}Si 2_1^+.

V. CONCLUSION

A reinvestigation of the n-rich ^{34}Al isotope and the logical next step, the study of ^{35}Al, was succesful with the 1 GeV pulsed proton beam on a thick U target at CERN. A detailed analysis of the beta decays leading to N=20 and 21 nuclei, ^{34}Si and ^{35}Si, was made to get a better understanding of the sd-fp shells interface. The ^{35}Si results have allowed the location of single-particle $p_{3/2}$ and $d_{3/2}$ states, giving an important reference point for extrapolation in shell-model calculations. From comparison of the experimental data with predicted GT transitions, it is concluded that all allowed transitions to bound levels have been observed. Additional information on levels of opposite parity to the β emitting levels, revealing the binding energy of the n$\hbar\omega$ excitation, was also obtained.

Further developments are seen in two directions :

- the extension to more exotic, N=21, isotopes. In this line, a first study of ^{33}Na $\rightarrow$ ^{33}Mg beta decay was made recently [41].

- the second one concerns future experiments allowing a better description of the GT strength leading to unbound states. The success of the shell-model calculation suggests the use of similar techniques for a complete exploration of the excitation range accessible in the decay process.

An evaluation of the contribution of higher terms in the n$\hbar\omega$ excitation of low-energy configurations will perhaps result from the comparison of the data with theory.

ACKNOWLEDGMENTS

This work was supported in part by the European Program of Training Mobility and Research.

---

[1] T. Motobayashi et al., Phys. Lett. B346, 9 (1995).
[2] R.W. Ibbotson et al., Phys. Rev. Lett. 80, 2081 (1998).
[3] P.L. Reeder, Y. Kim, W.K. Hensley, H.S. Miley, R.A. Warner, Z.Y. Zhou, D.J. Vieira, J.M. Wouters, and H.L. Siefert, Proc. Intern. Conf. on Exotic Nuclei and Atomic Masses, Arles, France, (1995), Eds. M. de Saint Simon and O. Sorlin, p.587 (1995).
[4] R.W. Ibbotson, T. Glasmacher, P.F. Mantica, and H. Scheit, Phys. Rev. C59, 642 (1999).
[5] F. Sarazin et al., Proc. of the XXXVII Int. Winter Meeting on Nuclear Physics, Bormio (1999).
[6] C. Thibault, R. Klapisch, C. Rigaud, A.M. Poskanzer, R. Prieels, L. Lessard, and W. Reisdorf, Phys. Rev. C12, 644 (1975).
[7] C. Detraz, D. Guillemaud, G. Huber, R. Klapisch, M. Langevin, F. Naulin, C. Thibault, L.C. Carraz, and F. Touchard, Phys. Rev. C19, 164 (1979).
[8] D. Guillemaud-Mueller, C. Detraz, M. Langevin, F. Naulin, M. de Saint-Simon, C. Thibault, F. Touchard, and M. Epherre, Nucl. Phys. A426, 37 (1984).
[9] G. Klotz, P. Baumann, M. Bounajma, A. Huck, A. Knipper, G. Walter, G. Marguier, C. Richard-Serre, A. Poves, and J. Retamosa, Phys. Rev. C47, 2502 (1993).
[10] G. Audi, O. Bersillon, J. Blachot, and A.H. Wapstra, Nucl. Phys. A624, 1 (1997).
[11] X. Campi, H. Flocard, A.K. Kerman, and S. Koonin, Nucl. Phys. A251, 193 (1975).

[12] A. Watt, R.P. Singhal, M.H. Storm, and R.R. Whitehead, J. Phys. G7, L145 (1981).
[13] B.H. Wildenthal, M.S. Curtin, and B.A. Brown, Phys. Rev. C28, 1343 (1983).
[14] A. Poves and J. Retamosa, Phys. Lett. B184, 311 (1987); Nucl. Phys. A571, 221 (1994).
[15] E.K. Warburton, J.A. Becker, and B.A. Brown, Phys. Rev. C41, 1147 (1990).
[16] K. Heyde and J.L. Wood, J. Phys. G17, 135 (1991).
[17] N. Fukunishi, T. Otsuka, and T. Sebe, Phys. Lett. B296, 279 (1992).
[18] T. Otsuka and N. Fukunishi, Phys. Rep. 264, 297 (1996).
[19] J. Retamosa, E. Caurier, F. Nowacki, and A. Poves, Phys. Rev. C55, 1266 (1997).
[20] E. Caurier, F. Nowacki, A. Poves, and J. Retamosa, Phys. Rev. C58, 2033 (1998).
[21] P. Baumann, A. Huck, G. Klotz, A. Knipper, G. Walter, G. Marguier, H.L. Ravn, C. Richard-Serre, A. Poves, and J. Retamosa, Phys. Lett. B228, 458 (1989).
[22] S. Nummela et al. , AIP Conf. Proc. Experimental Nuclear Physics in Europe, Sevilla, Spain (1999), Eds. B. Rubio, M. Lozano, W. Gelletly, p.55 (1999).
[23] S. Nummela et al., Proc. of the XXXVIII Int. Winter Meeting on Nuclear Physics, Bormio (2000).
[24] P. Baumann, M. Bounajma, F. Didierjean, A. Huck, A. Knipper, M. Ramdhane, G. Walter, G. Marguier, C. Richard-Serre, B.A. Brown, and the ISOLDE Collaboration, Phys. Rev. C58, 1970 (1998).
[25] W. Ziegert et al., Proc. of the 4th Int. Conf. on Nuclei far from Stability, CERN81-09, 327 (1981).
[26] M. Bounajma, Thesis, Strasbourg University (1996).
[27] B. Fornal et al., Phys. Rev. C49, 2413 (1994).
[28] L.K. Fifield, C.L. Woods, R.A. Bark, P.V. Drumm, and M.A.C. Hotchkis, Nucl. Phys. A440, 531 (1985).
[29] D. Bazin et al., AIP Conf. Proc. 5th Int. Conf. Nuclei far from Stability, Rosseau Lake, Canada (1987), Ed. I.S. Towner, p.722 (1988).
[30] D.H. Wilkinson, Nucl. Phys. A133, 1 (1969).
[31] D.H. Wilkinson, Nucl. Instr. Meth. 82 (1970).
[32] M. Lewitowicz et al., Nucl. Phys. A496, 477 (1989) and A.C. Mueller et al., Z. Phys. A330, 63 (1988).
[33] P.M. Endt, Nucl. Phys. A633, 1 (1998).
[34] P.M. Endt, At. Data Nucl. Data Tables 55, 17 (1993).
[35] D.J. Dean, M.T. Ressel, M. Hjorth-Jensen, S.E. Koonin, K. Langanke, and A.P. Zuker, Phys. Rev. C59, 2474 (1999).
[36] Y. Utsuno, T. Otsuka, T. Mizusaki, and M. Honma, Phys. Rev. C60, 054315 (1999).
[37] B.H. Wildenthal, Prog. Part. Nucl. Phys. 11,5 (1984).
[38] A. Poves and A. Zuker, Phys. Rep. 70, 4 (1981).
[39] S. Kahana, H.C. Lee, and C.K. Scott, Phys. Rev. 180, 956 (1969).
[40] F. Sarazin et al., Phys. Rev. Lett. (to be published).
[41] S. Nummela et al. (in preparation).

TABLE I. Energy and intensity of the gamma-rays attributed to the ^{34}Al decay.

Energy (keV)	Intensity[a] (relative)	Transition	
		from	to
124.21 (40)	51.9 (4.3)	4379	4255
590.85 (30)	7.7 (0.8)	4970	4379
928.98 (30)	103.9 (9.7)	4255	3326
1009.69 (40)	2.7 (0.4)	b)	
1052.76 (40)	3.9 (0.6)	4379	3326
1193.34 (20)	6.4 (0.8)	(3326	2133)
1434.86 (50)	13.9 (1.4)	b)	
1715.42 (80)	2.4 (0.4)	c)	
2696.43 (1.2)	4.8 (1.0)	c)	
3326.24 (1.6)	100	3326	0
4257 (3)	24.0 (3.8)	4255	0

a) Intensities are relative to the 3326 keV gamma-ray. The intensity per 100 beta decays is obtained by multiplying by a factor 0.55.

b) Corresponding to transitions in the ^{33}Si level scheme following neutron emission.

c) Unplaced in the decay scheme.

TABLE II. Beta intensities and logft values in the ^{34}Al β decay to bound levels in ^{34}Si.

E_x	I_β(%)	logft	J^π
0			0^+
2133.1 (5)	< 1	> 6.8	(0^+)
3326.4 (3)	< 12	> 5.5	2^+
4255.4 (5)	44 (4)	4.90 (6)	3^-
4379.5 (5)	26 (3)	4.90 (5)	$(4, 5)^-$
4970.4 (7)	4.2 (4)	5.70 (7)	$(4, 5)^-$

TABLE III. Energy and intensity of the gamma-rays attributed to the ^{35}Al decay.

Energy (keV)	Intensity[a] (relative)	Transition	
		from	to
64.05 (30)	100	974	910
124.20 (30)	2.5 (1.9)	b)	
910.11 (30)	99.7 (1.9)	910	0
929.12 (40)	5.8 (1.3)	b)	
973.78 (20)	11.8 (2.4)	974	0
1130.28 (40)	3.2 (0.9)		
1194.20 (40)	5.3 (1.2)	2168	974
2168.24 (60)	15.2 (3.1)	2168	0
3326.96 (70)	18.0 (3.6)	b)	
5629 (3)	2.4 (1.2)	c)	

a) Intensities are relative to the 64 keV gamma ray. The intensity per 100 beta decay is obtained by multiplying by a factor 0.45.

b) Corresponding to transitions in the ^{34}Si level scheme following neutron emission.

c) Unplaced in the decay scheme.

TABLE IV. Beta intensities and logft values in the ^{35}Al β decay to bound levels in ^{35}Si.

E_x (keV)	I_β (%)	logft	J $^\pi$
0	3.0 (10)	6.04 (14)	$(7/2^-)$
910.10 (30)	< 0.9	> 5.15	$(3/2^-)$
973.80 (30)	48 (9)	4.70 (8)	$(3/2^+)$
2168.10 (60)	9.2 (19)	5.22 (9)	$(5/2^-)$

TABLE V. Excitation energy of 2_1^+ in several nuclei and corresponding E2 transitions to the ground state. Values in parenthesis, from Ref. [19], are given for comparison.

nucleus	^{40}Ar	^{40}S	^{46}Ar	^{44}S	^{42}Si
E*(2^+)	1.37 (1.37)	0.98 (1.05)	1.53 (1.66)	1.22 (1.65)	1.49 (2.56)
BE2($2^+ \to 0^+$)	43 (43)	77 (75)	80 (90)	93 (79)	71 (49)

TABLE VI. ^{34}Si excitation energies (in MeV) and transition probabilities in e^2fm^4.

J^π	E_x in (MeV)		Transitions	B(E2$\uparrow$) in (e^2fm^4)	
	th. (this work)	exp.		th. (this work)	exp.
0_1^+	0.0	0.0	$0_1^+ \to 2_1^+$	118	85(33)[a]
0_2^+	2.6	(2.1)	$0_2^+ \to 2_1^+$	310	444(210)[b]
2_1^+	3.3	3.3	$0_1^+ \to 2_2^+$	104	< 104
2_2^+	5.4	5.3[c]			

a) from Ref. [2].

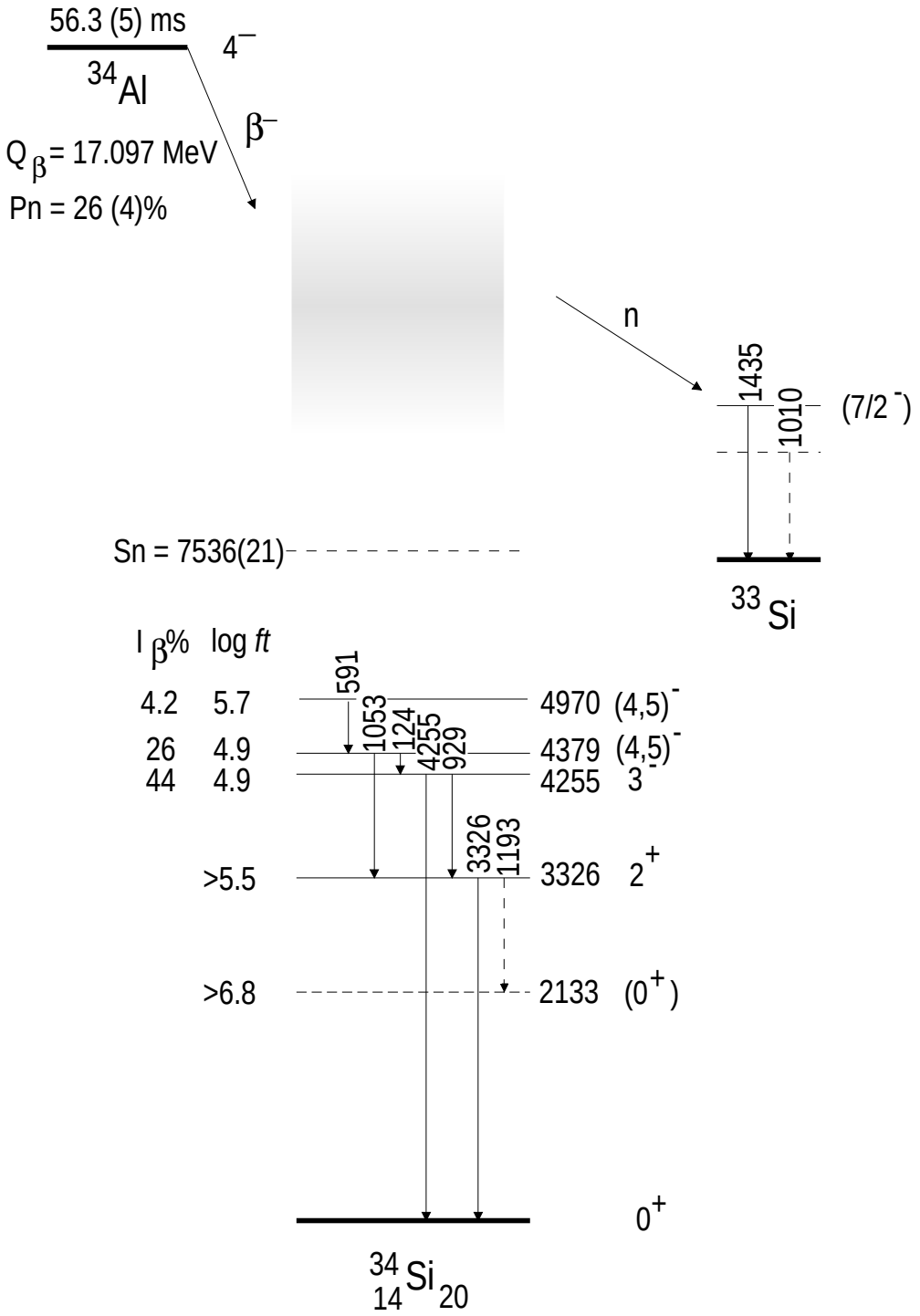

FIG. 1. ^{34}Al β-decay scheme.

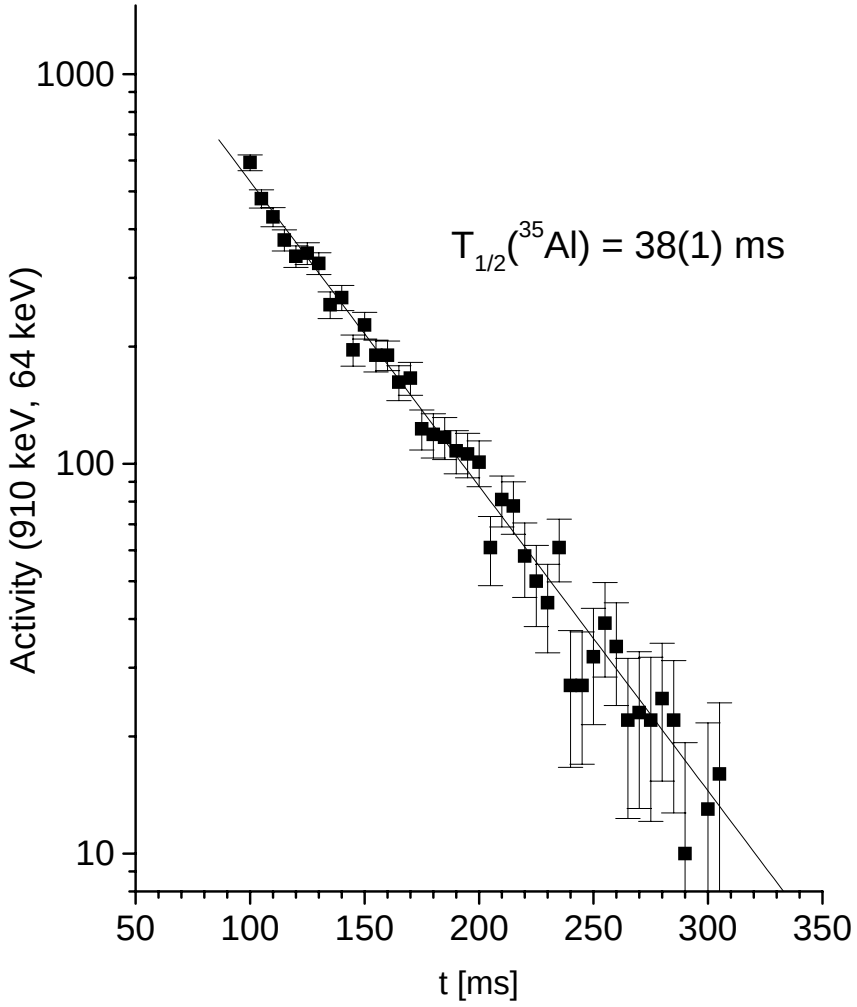

FIG. 2. Decay-time spectrum of the 64 and 910 keV lines. The result of the fit, which is indicated, has been combined with independent beta measurements to get the adopted value of ^{35}Al half-life : $T_{1/2}$=38.6(4) ms.

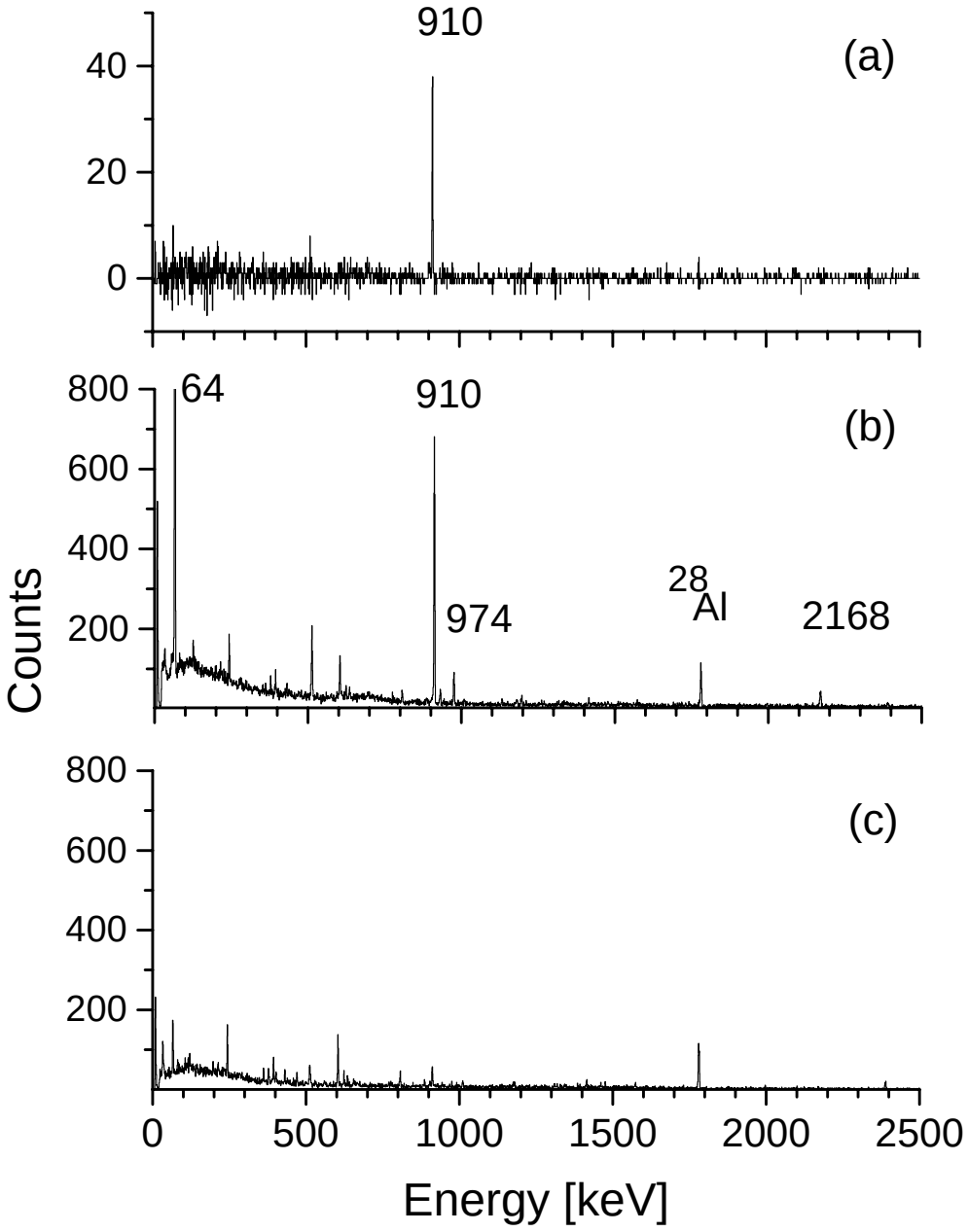

FIG. 3. Beta-delayed gamma spectrum obtained after collection of ^{35}Al. In the upper part (a), the gamma spectrum gated by the 64 keV. In (b) and (c), the gamma spectrum in coincidence with beta detection and registered in two time bins : 0-300 and 300-600 ms respectively, after collection.

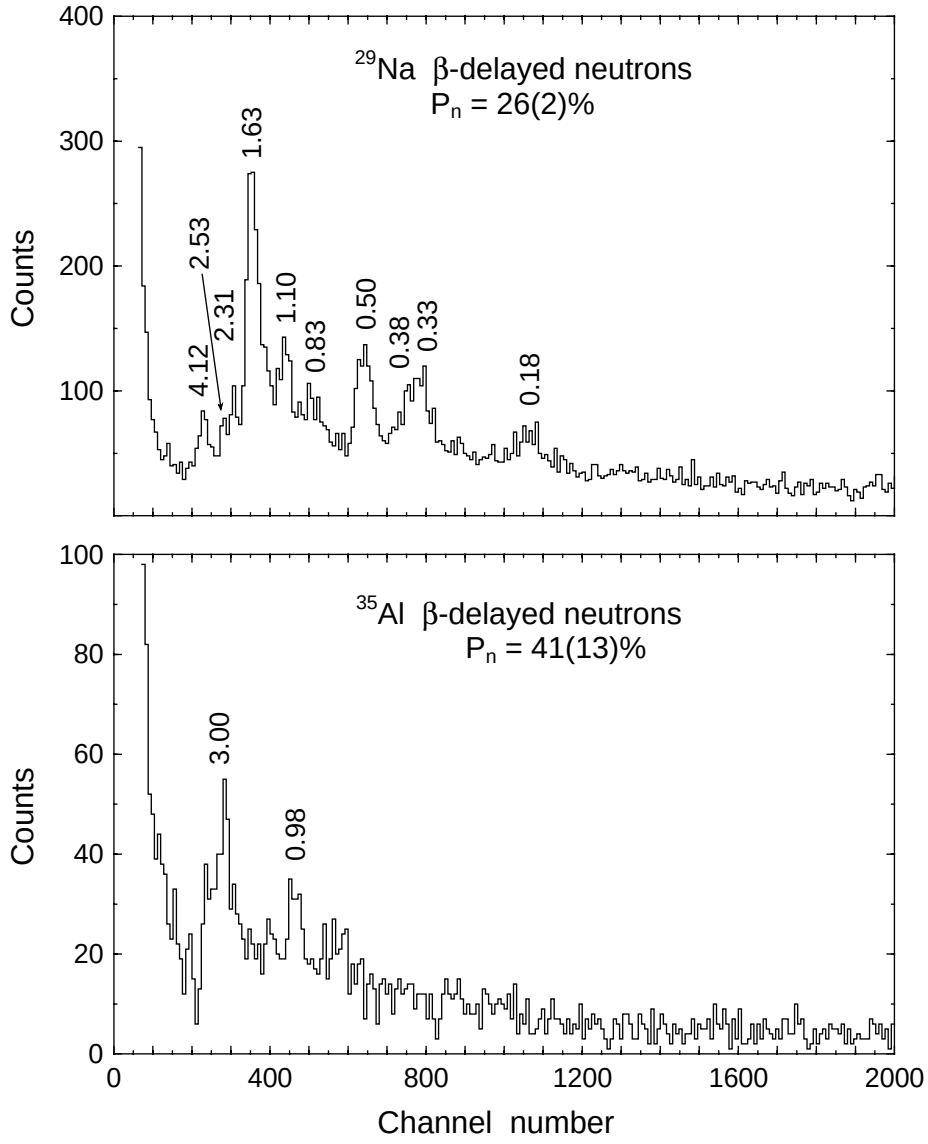

FIG. 4. Neutron time of flight spectrum taken in the identical conditions : with the ^{29}Na sources (upper part) and with the ^{35}Al nuclei (lower part). The time scale is 78 ps/channel.

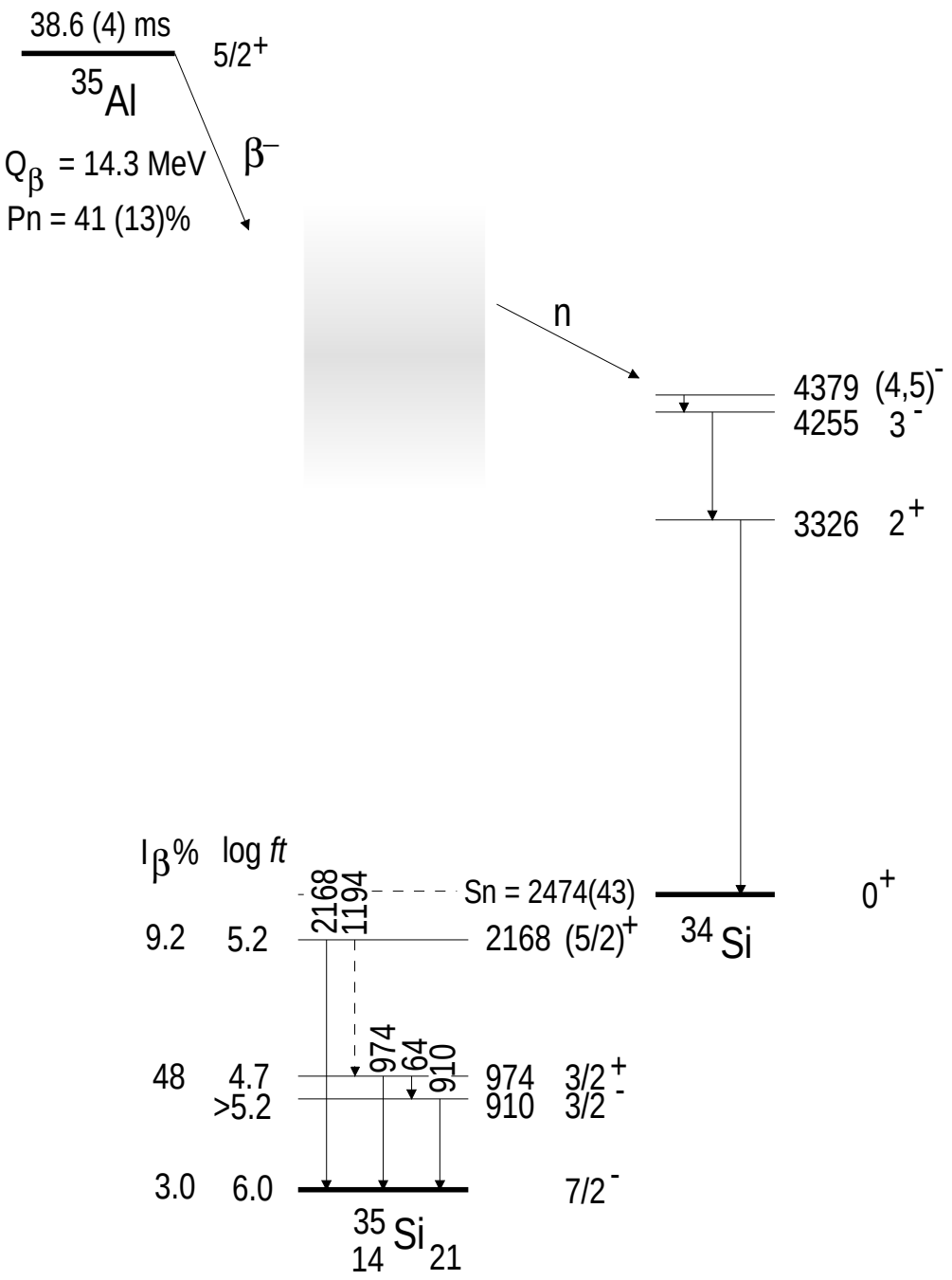

FIG. 5. ^{35}Al beta-decay scheme.

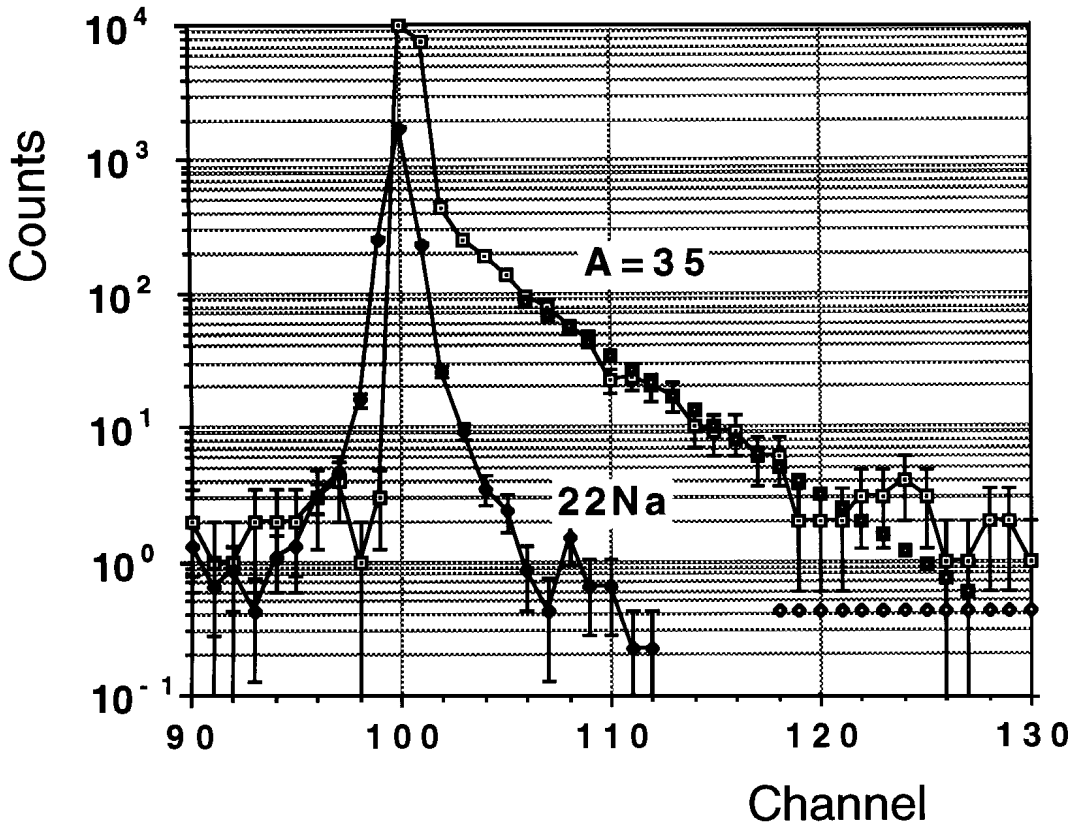

FIG. 6. Delayed coincidences taken in the decay of ^{35}Al with one plastic scintillator recording the betas and a BaF_2 detector for the gammas around 900 keV. After background substraction, the experimental curve is fitted by a single decay. Time scale : 2.03 ns/channel. ^{22}Na spectrum normalized in area to the A=35 delayed component.

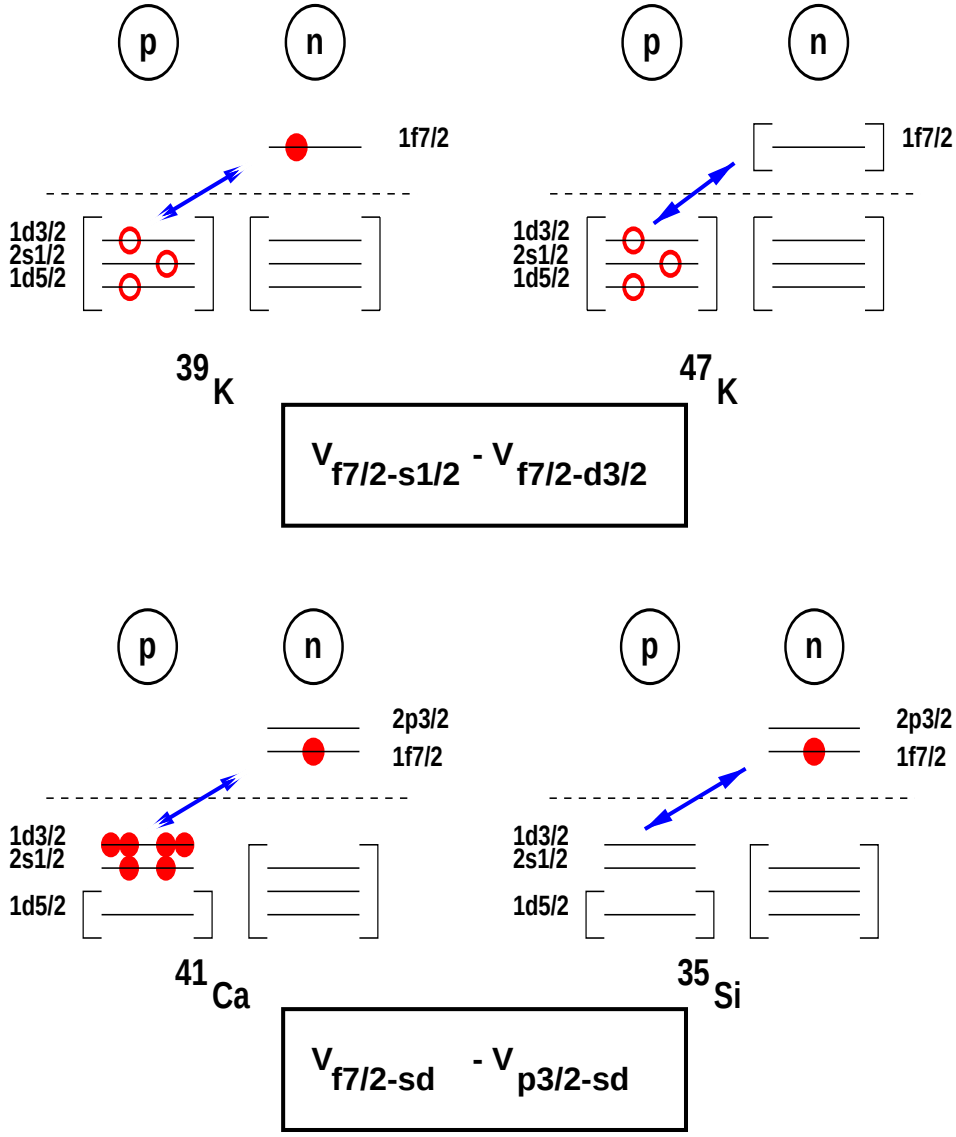

FIG. 7. In the upper part, proton-hole evolution with neutron filling in K isotopes.In the lower part, neutron-particle evolution with the decrease of proton number in N=21 isotones.

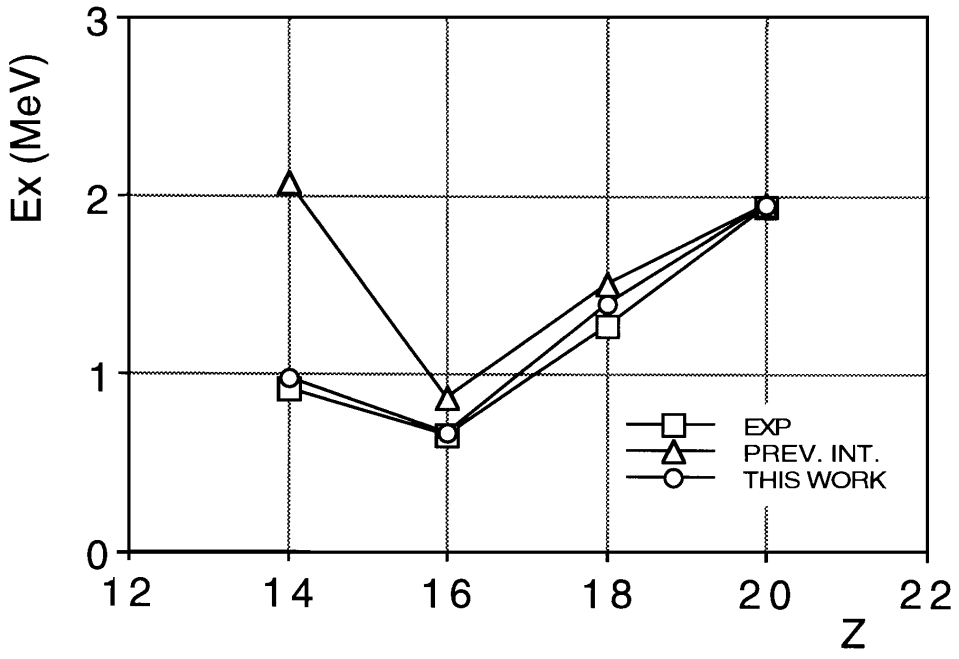

FIG. 8. Evolution of the $3/2^-$ excitation energy in N=21 isotones. The experimental values are compared with two calculations : first, with the set of parameters used prior to this experiment and finally, with the single-particle energy for Z=14 obtained in this work.

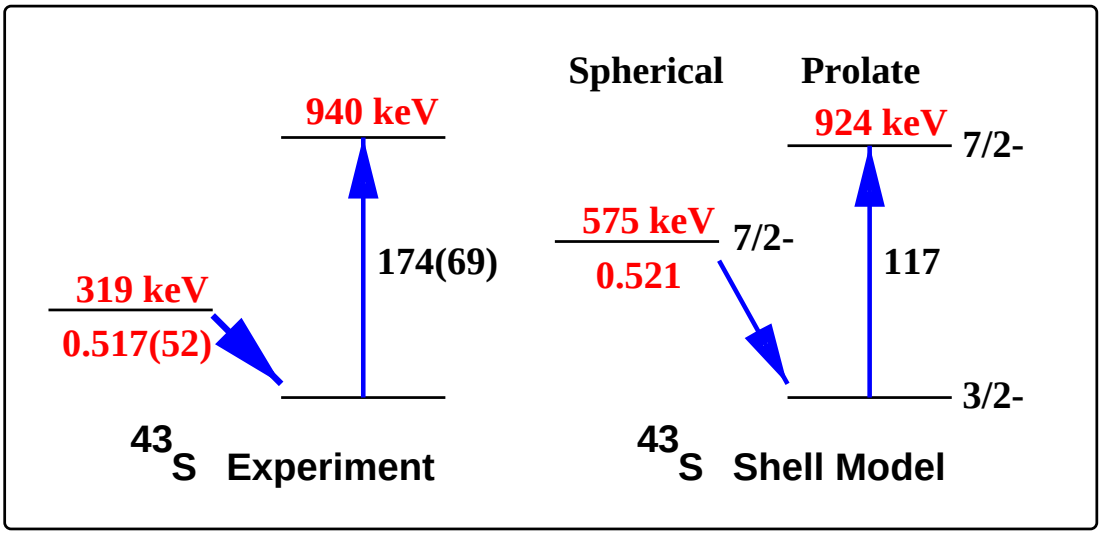

FIG. 9. First excited states in ^{43}S. Shell-model predictions are compared to experimental values (Refs. 4,5) ; numbers besides the transitions are B(E2) values in units of e^2fm^4.

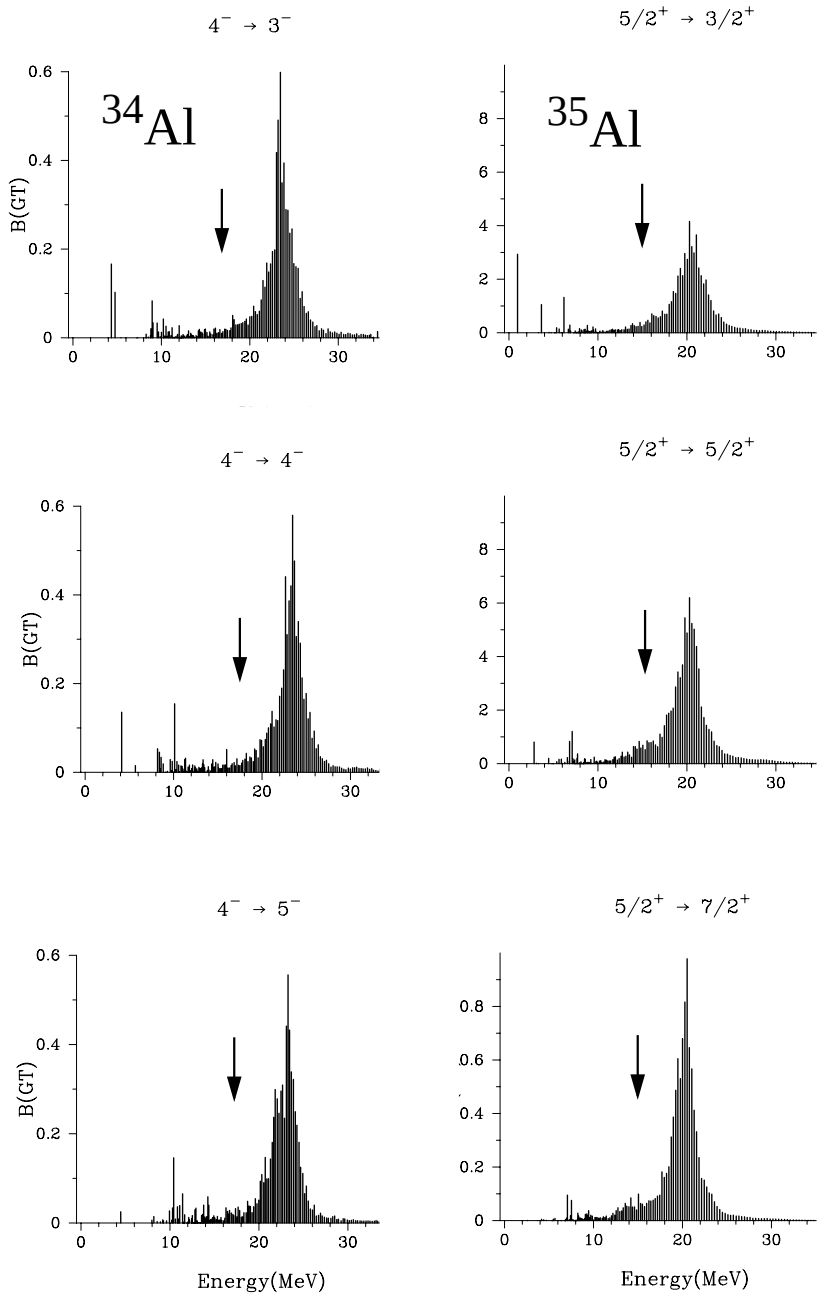

FIG. 10. Beta decay of ^{34}Al and ^{35}Al. Calculated values of Gamow-Teller strength distribution versus excitation energy in the final nucleus : ^{34}Si on the left and ^{35}Si on the right. The limit of the beta-decay window is indicated by the arrow.